

A Bit-Plane Decomposition Matrix-Based VLSI Integer Transform Architecture for HEVC

Honggang Qi, *Member, IEEE*, Qingming Huang, *Senior Member, IEEE*, and Wen Gao, *Fellow, IEEE*

Abstract—In this brief, a new very-large-scale integrated (VLSI) integer transform architecture is proposed for the High Efficiency Video Coding (HEVC) encoder. The architecture is designed based on the signed bit-plane transform (SBT) matrices, which are derived from the bit-plane decompositions of the integer transform matrices in HEVC. Mathematically, an integer transform matrix can be equally expressed by the binary weighted sum of several SBT matrices that are only composed of binary 0 or ± 1 . The SBT matrices are very simple and have lower bit width than the original integer transform in the form. The SBT matrices are also sparse and there are many zero elements. The sparse characteristic of SBT matrices is very helpful for saving the addition operators of SBT. In the proposed architecture, instead of the original integer transform in high bit width, the video data can be respectively transformed with the SBT matrices in lower bit width. As a result, the delay of the transform unit circuit can be significantly reduced with the proposed SBT. Moreover, exploiting the redundant element characteristic of SBT matrices, in which the elements are 0 or ± 1 , the adder reuse strategy is proposed for our transform architecture, which can save the circuit area efficiently. The simulation results show that by employing the proposed strategies the VLSI transform architecture can be synthesized in a proper area with a high working frequency and low latency. The architecture can support all HEVC encoders coding ultra high-definition video sequences in real time.

Index Terms—Bit-plane matrix, High Efficiency Video Coding (HEVC), integer transform, ultra high definition (HD), very-large-scale integrated (VLSI) architecture.

I. INTRODUCTION

DISCRETE cosine transform (DCT) is a key technology for video coding. It was first applied in image coding by Ahmed in 1974 [1]. After some decades, DCT was widely adopted as a video coding technology. Early video coding standards, such as JPEG [2], MPEG-2/H.262 [3], and H.263 [4], employed the real number DCT directly. The real number DCT has to be implemented in float point precision, which is high complexity with up to 64 bitwidth in digital system. It cannot be accepted to implement the real number DCT in so high bitwidth. For reducing the complexity of DCT implementation, the integer transforms, the approximated forms of real number DCT, are widely used in the actual encoders replacing the real number DCT. However, the integer transforms were not regulated in standards, which lead to error drifting problems so that greatly deteriorate decoded video. For solving this

problem, in the later video standards, such as H.264/Advanced Video Coding (AVC) [5], Audio and Video Standard (AVS) [6], and High Efficiency Video Coding (HEVC) [7], the explicit integer transforms are defined.

Transform is a frequently used module when compressing video; thus, the complexity of a transform has an important effect on the whole complexity of the video encoder. Chen *et al.* derived the factorization relationship between $N \times N$ and $N/2 \times N/2$ DCT matrices by analyzing the periodic property of the cosine function [8]. With the factorization relationship of DCT, the number of arithmetic operations of the transform can be reduced. Ahmed *et al.* [9] decomposed the DCT matrix into sparse submatrices where the multiplications are avoided by using the lifting scheme. Arai *et al.* [10] proposed an Arai, Agui, and Nakajima (AAN) fast algorithm based on the common factor extraction algorithm in which the complicated common factors were moved from the transform kernel to the scale part. Only five multipliers are required in AAN's transform kernel. The multiplier is expensive against the adder in the integration circuit. Thus, the multiplication operation is usually replaced by adders in the circuit design. Tsui and Chan [11] developed an efficient multiplierless fast Fourier transform (FFT)-like transform based on a recursive noise model that minimizes the hardware resources of the transform while maintaining the high performance. In [12], a multiplierless hardware implementation using a second-order cone programming technique is presented, and the dynamic ranges of intermediate data are minimized through geometric programming.

HEVC is the latest video coding with a higher coding performance than other existing ones. Many novel coding algorithms are introduced in HEVC. Particularly in the aspect of the transform, up to 32×32 integer transform is applied for improving coding performance. Theoretically, a large-size transform is usually efficient for coding a large-size prediction block and vice versa. However, the implementation complexity of a transform is increasing with the enlarging transform size. Thus, it is becoming more and more important for reducing the implementation complexity of a transform. The 32×32 transform is the most complex in the transforms of HEVC; thus, the improvement of the 32×32 transform also can be efficient for the whole transform circuit.

Many research works on transform implementation optimization for HEVC have been done in the past [13]–[15]. Meher *et al.* proposed an efficient constant matrix multiplication scheme to derive parallel architectures of a transform for HEVC [13], which can support the real-time ultra HD video codec. In [14], some simplification strategies, such as the reuse of transform structure and multiplierless implementation, were adopted for saving the hardware cost. The work in [15]

Manuscript received August 31, 2015; revised March 23, 2016; accepted May 27, 2016. Date of publication June 2, 2016; date of current version February 24, 2017. This work was supported in part by the National Science Foundation of China under Grants 61472388 and 61379100. This brief was recommended by Associate Editor C. Shing-chow.

The authors are with University of Chinese Academy of Sciences, Beijing 100049, China (e-mail: hqqi@ucas.ac.cn).

Digital Object Identifier 10.1109/TCSII.2016.2576061

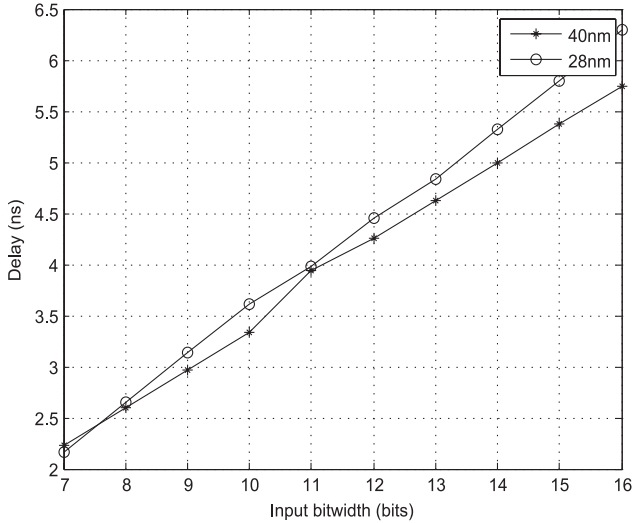


Fig. 1. Delay versus bit width of an adder implemented in 28- and 40-nm CMOS standard cell libraries.

presented a transform architecture that uses the canonical signed digit representation and common subexpression elimination technique to perform the multiplication with a shift-add operation. Based on these optimizations, the transform architecture is greatly simplified for practice application. However, with the increasing applications of high definition (HD) and ultra HD video coding, the higher processing capacity of codecs is required. Thus, all modules in video codec, including the transform, need to be further improved for real-time coding with low complexity.

The existing transform architectures consider how to reduce the number of arithmetic operators, such as addition and multiplication, more than the data bit width in the transform. In fact, the data bit width is also an important factor impacting on the circuit speed and area of VLSI architecture. A circuit with a large bit width needs a larger number of fan-in or fan-out of logic gate, and more MOS devices are required in the logic gate circuit. Thus, the capacitive load and resistance of the logic gate all increase with widening bit width. According to the first-order resistance and capacitance (RC) circuit model theory, the delay of the circuit is related with RC. Large RC leads to long circuit delay. The circuit delay varying with the increasing input bit width in two typical CMOS processes (SMIC40nm and GF28nm) is shown in Fig. 1. As for the adder, the carry chain is the critical path for the circuit delay, which is also dependent on the input and output bit width. Each extra bit increasing will lead to larger delay. Thus, aside from the number of arithmetic operations, the bit width is the other optimization factor for a fast transform architecture. In this brief, we propose a new VLSI architecture for the integer transforms of the HEVC standard for reducing the bit widths of data. The integer transform matrix is decomposed into several signed bit-plane transform (SBT) matrices that are used in the proposed architecture. Moreover, a number of adders are reused based on the redundant property of elements of bit matrices. With the bit matrix-based transform algorithm, the proposed VLSI transform architecture can process 32 pixels/cycle data throughput maximally with very high working frequency and proper area.

The rest of this brief is organized as follows. In Section II, the proposed transform bit-plane decomposition algorithm for optimizing the bit width of intermediate data is described and the adder reuse algorithm based on the transform bit-plane matrices for reducing the number of adders is introduced. Then, the proposed VLSI transform architecture is presented, and the simulation results are shown and discussed in Section III. Finally, we conclude this brief in Section IV.

II. SIGNED BIT MATRIX-BASED TRANSFORM ALGORITHM

A. Bit-Plane Decomposition of Integer Transform

In order to narrow the bit width of intermediate transformed data, we propose the bit decomposition algorithm which decomposes the integer transform matrix into several SBT matrices.

Let $d_{i,j}$ be the element in the i th row and j th column in the $N \times N$ integer transform matrix D_N , i.e., $D_N = (d_{i,j})$. If $d_{i,j}$ is positive, the binary expression of $d_{i,j}$ is $(b_{K-1,i,j}, \dots, b_{1,i,j}b_{0,i,j})_2$, $b_{k,i,j} \in \{0, 1\}$. Then, there is the relation

$$d_{i,j} = \sum_{k=0}^{K-1} (\text{sgn}(d_{i,j})b_{k,i,j}2^k), \quad b_{k,i,j} \in \{0, 1\} \quad (1)$$

where K is the number of binary significant bits of element $d_{i,j}$, $b_{k,i,j}$ denotes the k th bit of $d_{i,j}$, and $\text{sgn}(\ast)$ is the sign indication function that returns 1 for the positive value and -1 for the negative value, i.e., $\text{sgn}(x) = \begin{cases} 1, & x > 0 \\ -1, & x < 0 \end{cases}$. Thus, (1)

can also be rewritten as

$$d_{i,j} = \sum_{k=0}^{K-1} (b_{k,i,j}2^k), \quad b_{k,i,j} \in \{0, \text{sgn}(d_{i,j})\}. \quad (2)$$

Equation (2) is the signed integer binarization. If all elements $d_{i,j}$ in integer transform matrix D_N are binarized and all the k th bits of all binary $d_{i,j}$, $b_{k,i,j}$, $0 \leq i, j < N$, construct the k th bit plane, which is expressed in the form of $N \times N$ SBT matrix $B_{N,k} = (b_{k,i,j})$, there is

$$D_N = \sum_{k=0}^{K-1} (B_{N,k}2^k) \quad (3)$$

where K is the binary bit width of the maximum element in matrix D_N , i.e., $K = \lceil \log_2^{\max(d_{i,j})} \rceil$. The matrix $B_{N,k}$ containing elements of 0 or ± 1 is just the SBT matrix. K SBT matrices are totally generated in the matrix decomposition. Equation (3) specifies the bit-plane decomposition from an $N \times N$ integer transform matrix D_N to K $N \times N$ SBT matrices $B_{N,k}$.

Letting X_N be the $N \times N$ matrix of input data, according to the bit-plane decomposition (3), the integer transform can be equally expressed by the weighted sum of K SBTs as

$$D_N X_N = \sum_{k=0}^{K-1} (B_{N,k}2^k X_N) = \sum_{k=0}^{K-1} (B_{N,k} X_N 2^k) \quad (4)$$

where $B_{N,k} X_N$ is the k th SBT of input data X_N . Equation (4) specifies that the integer transform can be replaced by K SBTs. The final result of the integer transform can be equally obtained

through weighting (multiplied by 2^k) and accumulating the output data of each SBT as described in (4).

Compared with integer transform matrix D_N , the SBT matrices $B_{N,k}$ are simple, only including elements of 0 and ± 1 . An example for the HEVC 8×8 integer transform D_8 and its sixth SBT matrix $B_{8,6}$ is shown as

$$D_8 = \begin{pmatrix} 90 & 87 & 80 & 70 & 57 & 43 & 25 & 9 \\ 87 & 57 & 9 & -43 & -80 & -90 & -70 & -25 \\ 80 & 9 & -70 & -87 & -25 & 57 & 90 & 43 \\ 70 & -43 & -87 & 9 & 90 & 25 & -80 & -57 \\ 57 & -80 & -25 & 90 & -9 & -87 & 43 & 70 \\ 43 & -90 & 57 & 25 & -87 & 70 & 9 & -80 \\ 25 & -70 & 90 & -80 & 43 & 9 & -57 & 87 \\ 9 & -25 & 43 & -57 & 70 & -80 & 87 & -90 \end{pmatrix} \quad (5)$$

$$B_{8,6} = \begin{pmatrix} 1 & 1 & 1 & 1 & 0 & 0 & 0 & 0 \\ 1 & 0 & 0 & 0 & -1 & -1 & -1 & 0 \\ 1 & 0 & -1 & -1 & 0 & 0 & 1 & 0 \\ 1 & 0 & -1 & 0 & 1 & 0 & -1 & 0 \\ 0 & -1 & 0 & 1 & 0 & -1 & 0 & 1 \\ 0 & -1 & 0 & 0 & -1 & 1 & 0 & -1 \\ 0 & -1 & 1 & -1 & 0 & 0 & 0 & 1 \\ 0 & 0 & 0 & 0 & 1 & -1 & 1 & -1 \end{pmatrix} \quad (6)$$

As to the matrix multiplication used in the transform, if the maximum bit width of input data is n bits, the maximum bit width of the output data of the $N \times N$ 1-D transform, $D_N X$, should be $n + \lceil \log_2^{\max(\sum_{j=0}^{N-1} |d_{i,j}|)} \rceil$. However, the maximum bit width of the output data of the k th SBT, $B_{N,k} X_N$, should be $n + \lceil \log_2^{\max(\sum_{j=0}^{N-1} |d_{k,i,j}|)} \rceil$. Due to $d_{k,i,j} \in \{0, 1, -1\}$, the maximum bit width of the output data is no more than $n + \lceil \log_2^N \rceil$. It is easy to be known that $\lceil \log_2^{\sum_{j=0}^{N-1} |d_{i,j}|} \rceil \gg \lceil \log_2^{\sum_{j=0}^{N-1} |d_{k,i,j}|} \rceil$.

Applying the proposed SBT algorithm to the transform architecture, instead of the integer transform matrix circuits, the SBT matrix circuits are implemented and the input data are transformed with each SBT matrix circuit, respectively. Due to the simple elements of SBT matrices, the bit widths of intermediate transformed data and output data are significantly reduced. The bit width of output data should be $n + \lceil \log_2^N \rceil$ maximally. Taking the 32×32 1-D integer transform as an example, the increasing bit width of output data is only 5 b with the SBT algorithm, compared with the 11-b increasing of the straightforward integer transform. The bit widths of SBT increase slowly as the intermediate data are processed stage by stage, which shortens the circuit delay and constrains the clock cycle to be smaller. Although the delay of the integer transform circuit is reduced based on the proposed bit transform algorithm, more adders are required due to more SBTs. However, the bit widths of adders used in SBT are also so low that the addition operation is also very fast. Additionally, It can be observed from (6) that many zero elements are in the SBT matrix. The number of actually required addition operations is seldom due to the sparse SBT matrix according to the rule of matrix multiplication. The sparse characteristic of the SBT matrices can benefit for reducing the addition operations in the transform process.

The SBT matrix only contains elements 0 and ± 1 . There are many addition operation redundancies in SBT. Thus, we propose the adder reuse method based on the element redundancy characteristic of SBT matrices for reducing the number of adders in the next section.

B. Adder Reuse Based on SBT Matrices

If the input data are organized in the form of an N -dimension column vector, i.e., $\vec{x} = (x_0, x_1, \dots, x_{N-1})^T$, the 1-D transform of the input data vector can be expressed as

$$D_N \cdot \vec{x} = \begin{pmatrix} \vec{d}_0 \\ \vec{d}_1 \\ \vdots \\ \vec{d}_{N-1} \end{pmatrix} \cdot \vec{x} = \begin{pmatrix} \vec{d}_0 \cdot \vec{x} \\ \vec{d}_1 \cdot \vec{x} \\ \vdots \\ \vec{d}_{N-1} \cdot \vec{x} \end{pmatrix} \quad (7)$$

where $\vec{d}_i = (d_{i,0}, d_{i,1}, \dots, d_{i,N-1})$ is an N -dimension row vector which is the i th row elements in transform matrix D_N , and $\vec{d}_i \cdot \vec{x} = d_{i,0}x_0 + d_{i,1}x_1 + \dots + d_{i,N-1}x_{N-1}$. Due to $(d_{i,j})_{10} = (b_{K-1,i,j}, \dots, b_{1,i,j}, b_{0,i,j})_2$, the k th SBT is

$$B_{N,k} \cdot \vec{x} = \begin{pmatrix} \vec{b}_{k,0} \\ \vec{b}_{k,1} \\ \vdots \\ \vec{b}_{k,N-1} \end{pmatrix} \cdot \vec{x} = \begin{pmatrix} \vec{b}_{k,0} \cdot \vec{x} \\ \vec{b}_{k,1} \cdot \vec{x} \\ \vdots \\ \vec{b}_{k,N-1} \cdot \vec{x} \end{pmatrix} \quad (8)$$

where $\vec{b}_{k,i} = (b_{k,i,0}, b_{k,i,1}, \dots, b_{k,i,N-1})$ and $\vec{b}_{k,i} \cdot \vec{x} = b_{k,i,0}x_0 + b_{k,i,1}x_1 + \dots + b_{k,i,N-1}x_{N-1}$. If the dimension of vector $\vec{b}_{k,i}$ is small, it is very probable that $\vec{b}_{k,i} \cdot \vec{x} = \vec{b}_{k,j} \cdot \vec{x}$. There are many potentially redundant addition operations in $\vec{b}_{k,i} \cdot \vec{x}$, $0 \leq i < N$. Thus, it is reasonable that the adder reuse is efficiently explored in small dimensional vector $\vec{b}_{k,i}$. However, the dimension of \vec{x} is usually not very small, such as 16 or 32, which prevents from exploring the element redundancy characteristics of SBT. In the proposed adder reuse method, the SBT $\vec{b}_{k,i} \cdot \vec{x}$ is split into L parts of sub-SBT $\vec{b}_{k,i}^l \cdot \vec{x}^l$ ($0 \leq l < L$), and their relationship is

$$\vec{b}_{k,i} \cdot \vec{x} = \sum_{l=0}^{L-1} (\vec{b}_{k,i}^l \cdot \vec{x}^l) \quad (9)$$

where the number of elements in vector \vec{x}^l is M , i.e., $\dim(\vec{x}^l) = M$ ($M = N/L$, only considering N divided exactly by L), $\vec{b}_{k,i}^l = (b_{k,i,lM}, b_{k,i,lM+1}, \dots, b_{k,i,(l+1)M-1})$, and $\vec{x}^l = (x_{lM}, x_{lM+1}, \dots, x_{(l+1)M-1})^T$. $\vec{b}_{k,i}^l \cdot \vec{x}^l$ is named as M -dimension sub-SBT (M -SSBT), and the vector $\vec{b}_{k,i}^l$ is named as M -SSBT vector. Through the split of the SBT matrix, the SSBT with a small dimension is obtained. The situations of element combinations in $\vec{b}_{k,i}^l$ decide the number of adders. The number of all the possible element combinations of the M -SSBT vector is α^M , where α denotes the number of all the possible values of an element in the vector. For vector $\vec{b}_{k,i}^l$ from the SBT matrix, $b_{k,i,j} \in \Phi = \{0, 1, -1\}$, $\alpha = |\Phi| = 3$, where $|\Phi|$ is the cardinality of set Φ . For reusing adders more efficiently, the M should be smaller. In this architecture, let $M = 2$, i.e., $\dim(\vec{b}_{k,i}^l) = 2$. The SBT vector is divided

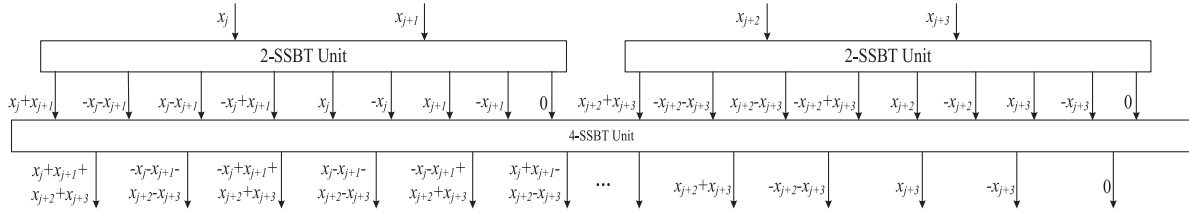


Fig. 2. Hierarchical structure of SBT.

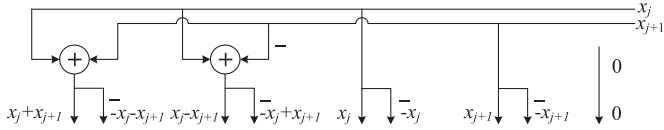


Fig. 3. Adder reuse circuit of 2-SSBT.

into multiple 2-SSBT vectors. The number of all the possible element combination situations of 2-SSBT is $3^2 = 9$. The nine element combinations are (1, 1), (1, -1), (-1, 1), (-1, -1), (1, 0), (-1, 0), (0, 1), (0, -1), and (0, 0). As for the 2-SSBT vector, all possible addition operations for $\vec{b}_{k,i}^l \cdot \vec{x}^l$ can be expressed as

$$\begin{pmatrix} 1 & 1 \\ 1 & -1 \\ -1 & 1 \\ -1 & -1 \\ 1 & 0 \\ -1 & 0 \\ 0 & 1 \\ 0 & -1 \\ 0 & 0 \end{pmatrix} \cdot \begin{pmatrix} x_j \\ x_{j+1} \end{pmatrix} = \begin{pmatrix} x_j + x_{j+1} \\ x_j - x_{j+1} \\ -x_j + x_{j+1} \\ -x_j - x_{j+1} \\ x_j \\ -x_j \\ x_{j+1} \\ -x_{j+1} \\ 0 \end{pmatrix}. \quad (10)$$

It can be seen from (10) that four adders are required in the subtransform of 2-SSBT. In fact, considering the relationship of positive and negative signs, all the additions of a 2-SSBT are done with only two adders. The adders used in the additions $i_x + i_{x+1}$ and $i_x - i_{x+1}$ can be reused by the additions $-(i_x + i_{x+1})$ and $-(i_x - i_{x+1})$, respectively, with two extra negative operators. The negative operator, which is implemented through reversing each bit and then adding 1, is very simple compared with the addition operator with negligible circuit implementation cost. Exploring the addition redundancy of the 2-SSBT vector, two adders are really required for computing $\vec{b}_{k,i}^l \cdot \vec{x}^l$. The inner circuit design of the 2-SSBT unit is described in Fig. 2.

According to the relationship between M -SSBT and $M/2$ -SSBT, the SBT can be implemented in a hierarchical way. An M -SSBT can be implemented through jointing two $M/2$ -SSBTs. The hierarchical structure of 4-SSBT as an example is illustrated in Fig. 3 where the output of two 2-SSBT units is input to a 4-SSBT unit for 4-SSBT computation. The inner circuit design of the 4-SSBT circuit is also shown in Fig. 4.

It can be summarized that the number of adders, #ADDER, used in the proposed adder reuse scheme for SBT can be calculated according to the expression

$$\#ADDER = \frac{\alpha^M - 1}{2} - \left(\alpha^{\frac{M}{2}} - 1 \right). \quad (11)$$

Taking 2-SSBT as an example, $M = 2$, and $\alpha = 3$; thus, the number of adders of a 2-SSBT is 2.

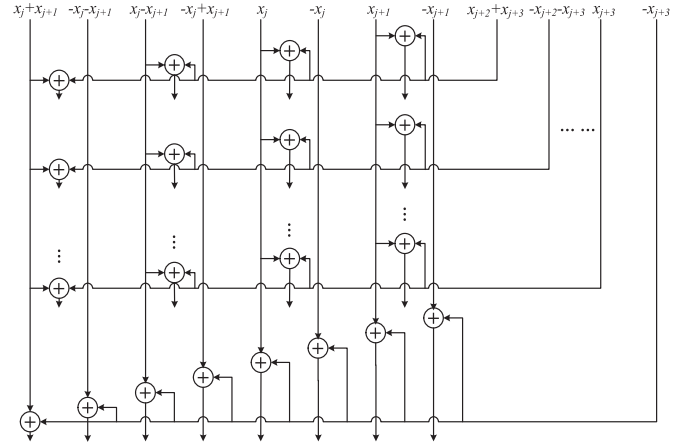


Fig. 4. Part of the adder reuse circuit of 4-SSBT.

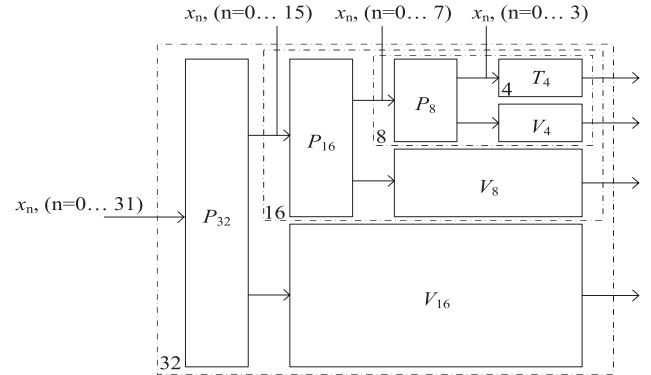


Fig. 5. One-dimensional 32x32 transform top-level architecture.

III. VLSI ARCHITECTURE AND SIMULATION RESULTS

HEVC adopts several integer transforms in different sizes from 4×4 to 32×32 , which are integrated in the proposed transform VLSI architecture. The transform architecture is implemented based on Chen's transform framework [10]. Chen proposed a fast DCT algorithm based on the factorization framework that N -point II-type DCT T_N can be recursively factorized into a $N/2$ -point II-type DCT $T_{N/2}$ and a $N/2$ -point IV-type DCT $V_{N/2}$. The transform in size N is decomposed into transforms in size $N/2$ recursively. The 32×32 1-D transform architecture based on Chen's fast transform algorithm is illustrated in Fig. 5, which is the top-level architecture of the proposed 1-D transform architecture. The SBT algorithm and corresponding adder reuse algorithm are incorporatively implemented in each $N \times N$ transform unit in Fig. 5. For implementing the 2-D transform, two 1-D transforms are implemented and connected, respectively, by a transpose buffer. Meher's transpose buffer solution [13] is employed in our 2-D

TABLE I
COMPARISONS BETWEEN EXISTING AND PROPOSED 1-D DCT ARCHITECTURES

Architecture	Technology (nm)	Gate counts (10 ³)	MAX Working frequency (MHz)	Max Throughput (ppc)	Decoding capability
Meher's[13]	90	131	187	16	7680x4320@60fps
Zhao's[14]	45	206	333	32	4096x2048@30fps
Darji's[15]	90	149	100	16	-
Proposed	40	255	450	32	7680x4320@60fps
Proposed	28	223	700	32	7680x4320@60fps

transform architecture. The transpose buffer is designed to be capable of pipelining the data with only several initial latency cycles, which can guarantee that the 2-D transform circuit is the same throughput with the 1-D transform circuit. The proposed 1-D transform architecture is synthesized with SMIC40nm and GF28nm CMOS standard cell libraries, which is compared with existing solutions of transform circuits [13]–[15]. The compared results are shown in Table I. In this table, the circuit area is estimated from the number of transistors by normalizing with respect to a basic two-input NAND gate. The synthesized results show that, with the 16-b input data, the proposed architecture costs about 255 K logic gates in the maximum working frequency of 450 MHz in a 40-nm CMOS process and 223 K logic gates in the maximum working frequency of 700 MHz in a 28-nm CMOS process. The high frequency is achieved from the optimized intermediate data with narrower bit width. The working frequency can be further improved through optimizing the critical paths at the cost of increasing circuit area. It can be easily compared from the simulation results that the proposed 1-D DCT architecture has almost as many as twice the gate count and significant higher working frequency than Meher's [13] and Darji's [15] and has comparable circuit area and stronger coding capability than Zhao's [14]. High working frequency means that the proposed transform circuit can synchronize to other high-frequency modules in the video encoder. The working frequency of the encoder modules has to be very high for the real-time coding of ultra HD video.

IV. CONCLUSION

A fast integer transform VLSI architecture-based sparse SBT is proposed for real-time ultra HD video coding conforming to the HEVC standard. Considering the bit width effect on circuit delay, the bit width of the integer transform matrix is optimized in the proposed VLSI architecture. The integer transform matrix with high-bit-width elements is decomposed into several SBT matrices with low-bit-width elements based on the proposed matrix bit-plane decomposition method. The transform architecture with the SBT algorithm can work more efficiently for the low-bit-width computations. The circuit reuse strategy is particularly proposed for the SBT to reduce the

number of adders of the VLSI architecture. A large number of adders for the SBT is saved using the proposed circuit reuse strategy. The proposed transform hardware architecture can process video data with higher speed and proper area compared with previous work.

REFERENCES

- [1] N. Ahmed, T. Natarajan, and K. R. Rao, "On image processing and a discrete cosine transform," *IEEE Trans. Comput.*, vol. C-23, no. 1, pp. 90–93, Jan. 1974.
- [2] G. K. Wallace, "JPEG still image data compression standard," *Commun. ACM*, vol. 34, no. 4, pp. 30–44, Apr. 1991.
- [3] "Generic coding of moving pictures and associated audio information Part 2: Video ITU-T and ISO/IEC JTC1," in *ITU-T Recommendation H.262, ISO/IEC 13818-2 (MPEG-2)*, Nov. 1994.
- [4] "Video coding for low bit-rate communication Version 1," in *ITU-T Recommendation H.263*, Nov. 1995.
- [5] T. Wiegand, G. Sullivan, G. Bjontegaard, and A. Luthra, "Overview of the H.264/AVC video coding standard," *IEEE Trans. Circuits Syst. Video Technol.*, vol. 13, no. 7, pp. 560–576, Jul. 2003.
- [6] L. Yu, S. Chen, and J. Wang, "Overview of AVS-video coding standards," *Signal Process., Image Commun.*, vol. 24, no. 4, pp. 247–262, Apr. 2009.
- [7] G. Sullivan, J.-R. Ohm, W.-J. Han, and T. Wiegand, "Overview of the high efficiency video coding (HEVC) standard," *IEEE Trans. Circuits Syst. Video Technol.*, vol. 22, no. 12, pp. 1649–1668, Dec. 2012.
- [8] W.-H. Chen, C. H. Smith, and S. C. Fralick, "A fast computational algorithm for the discrete cosine transform," *IEEE Trans. Commun.*, vol. COM-25, no. 9, pp. 1004–1009, Sep. 1977.
- [9] A. Ahmed, M. U. Shahid, and A. ur Rehman, "N-point DCT VLSI architecture for emerging HEVC standard," *VLSI Design*, vol. 2012, 2012, Art. no. 752024.
- [10] Y. Arai, T. Agui, and M. Nakajima, "A fast DCT-SQ scheme for images," *Trans. IEICE*, vol. E71, no. 11, pp. 1095–1097, Nov. 1988.
- [11] K. M. Tsui and S. C. Chan, "Error analysis and efficient realization of the multiplierless FFT-like transformation (ML-FFT) and related sinusoidal transformations," *J. VLSI Signal Process. Syst.*, vol. 44, no. 1–2, pp. 97–115, Aug. 2006.
- [12] S. H. Zhao and S. C. Chan, "Design and multiplierless realization of digital synthesis filters for hybrid-filter-bank A/D converters," *IEEE Trans. Circuits Syst. I, Reg. Papers*, vol. 56, no. 10, pp. 2221–2233, Oct. 2009.
- [13] P. K. Meher, S. Y. Park, B. K. Mohanty, K. S. Lim, and C. Yeo, "Efficient integer DCT architectures for HEVC," *IEEE Trans. Circuits Syst. Video Technol.*, vol. 24, no. 1, pp. 168–178, Jan. 2014.
- [14] W. Zhao, T. Onoye, and T. Song, "High-performance multiplierless transform architecture for HEVC," in *Proc. IEEE Int. Symp. Circuits Syst.*, May 2013, pp. 1668–1671.
- [15] A. D. Darji and R. P. Makwana, "High-performance multiplierless DCT architecture for HEVC," in *Proc. IEEE Int. Symp. VLSI Design Test*, Jun. 2015, pp. 1–5.